

# Experimental report

21/10/2022

**Proposal:** CRG-2614

**Council:** 4/2019

**Title:** Orbital currents in the two-leg CuO ladders cuprates

**Research area:**

**This proposal is a new proposal**

**Main proposer:** Dalila BOUNOUA

**Experimental team:** Lucile MANGIN-THRO

Dalila BOUNOUA

Yvan SIDIS

Marine VERSEILS

Victor BALEDENT

**Local contacts:** Frederic BOURDAROT

**Samples:** Sr14Cu24O41

Instrument	Requested days	Allocated days	From	To
IN22	8	8	11/02/2020	19/02/2020
IN3	1	1	10/02/2020	11/02/2020

**Abstract:**

# Orbital magnetism in two-leg ladder cuprate

The family of the two-leg spin  $\frac{1}{2}$  ladder cuprates  $\text{Sr}_{(14-x)}\text{Ca}_x\text{Cu}_{24}\text{O}_{41}$  (hereafter: SCCO- $x$ ) has attracted a lot of interest, owing to the emergence of superconductivity upon substitution [1]. The Ca-free compound  $\text{Sr}_{14}\text{Cu}_{24}\text{O}_{41}$  is a quasi-1D system, which consists of two interpenetrating subsystems of  $\text{CuO}_2$  chains and  $\text{Cu}_2\text{O}_3$  two-leg ladders. It realizes an intrinsically hole-doped compound with an effective charge of +2.25 per Cu (mixed valence  $\text{Cu}^{2+/\beta+}$ ), where the holes are located within the chains subsystem. Substitution with  $\text{Ca}^{2+}$  on the  $\text{Sr}^{2+}$  site results in a transfer of the holes carriers from the chains to the ladders subsystem [2]. Ca-doping results in a rich P-T phase diagram with various phases: spin liquid state, antiferromagnetic state, charge density wave, superconductivity under pressure [3]. A long-range ordered antiferromagnetic (AF-LRO) phase was also reported for  $x \geq 9$ . The origin of the AF-LRO is however still unclear. Indeed, while it was attributed to AF ordering within the chains, it was also proposed to originate from AF spin ordering within the ladders [4-5]. To account for such an AF state, one needs to elaborate a very complex magnetic pattern made of a large number of Cu spins.

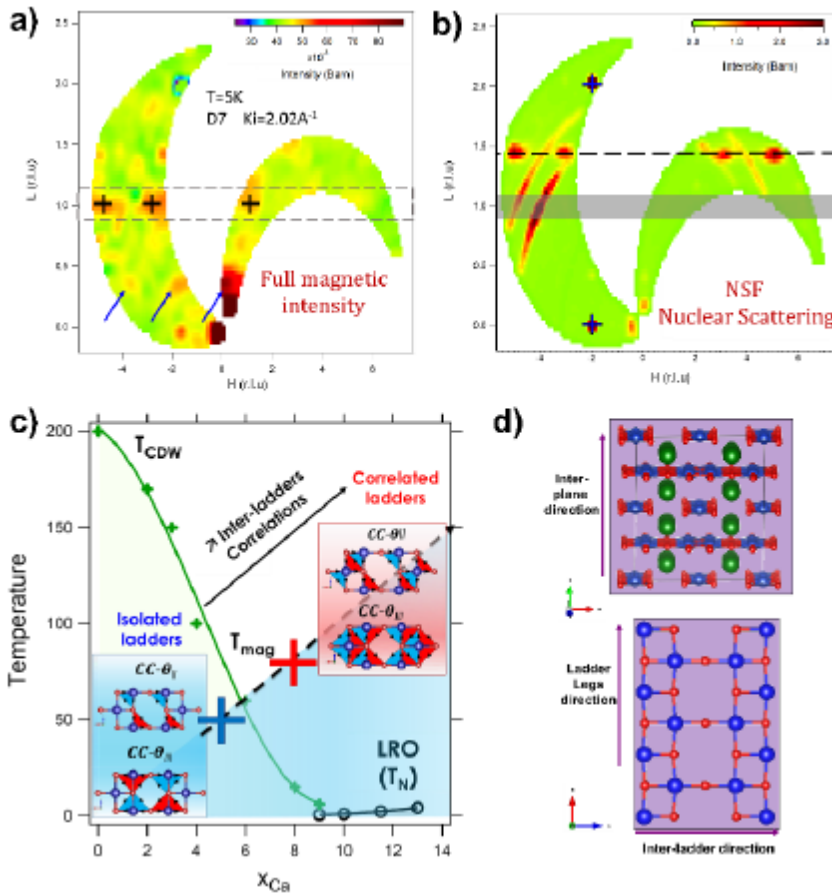


Figure 1 (a) SCCO-8: Mapping of the full magnetic scattering at 5K, deduced from XYZ-PA on D7. The map is given in r.l.u of the ladders subsystem and the intensities in mbarn. The area bounded by dashed lines indicates the ladder scattering ridge along  $(H,0,1)$  with magnetic spots located by crosses. The blue arrows show the satellite magnetic reflections. (b) SCCO-8: Mapping of nuclear intensity measured in the NSF channel. Spots at integer  $H$  and  $L$  values correspond to the nuclear scattering associated with the ladders, whereas the dashed lines are associated with the chains nuclear response. (c) Schematic phase diagram showing the evolution of the LC pattern as a function of the hole-doping (i.e. Ca-content). At large doping, inter-ladders correlations set-in and  $T_{\text{mag}}$  (crosses) increases. In heavily doped samples, an AFM-LRO further develops below  $T_{\text{N}}$  of a few Kelvin. Insets: (Up)  $\text{CC}\beta$ -II like model of LCs within one ladder unit cell with two staggered Cu-O orbital currents per Cu site flowing clockwise (red triangles) and anticlockwise (blue triangles). (Down)  $\text{CC}\beta$ -III model of LCs, as derived from a spin liquid initial state [3], within the ladder cell consisting of two counter-propagating currents flowing between oxygen sites. (d) Up: Crystal structure of SCCO (Cu in blue, O in red and Sr in green). Down:  $[a,c]$  plane projection of the ladders planes. [6].

We have revisited the magnetic properties of SCCO- $x$ , using polarized neutron diffraction (PND) [6]. Our PND measurements in two different SCCO single crystals with Ca doping levels  $x=5$  and  $8$ , using two different instruments (The cold-TAS 4F1 and the multi-detector diffractometer D7), equipped with distinct neutron polarization set-ups and operating with 2 distinct neutron wavelengths ( $k_i=2.57\text{\AA}^{-1}$  for 4F1 and  $k_i=2.02\text{\AA}^{-1}$  for D7). For both samples, PND measurements show the onset of a new magnetism. This one is at short range and preserves the lattice translational invariance ( $\mathbf{q}=0$  magnetism). It further gives rise to scattering on top of Q-positions where no nuclear scattering is expected from space-group symmetry selection rules [7] (Fig.1.a.b). The characteristic onset temperature for the magnetic correlations was found to be  $T_{\text{mag}}=50\text{K}$  and  $80\text{K}$  for SCCO-5 and SCCO-8 (Fig.1.c), respectively. At low Ca

content, only the magnetic response of one single isolated ladder is measured (SCCO-5:  $\xi_c \sim 20 \text{ \AA}$ , along the ladders legs and no correlation along a, the ladders rungs, Fig.1.d), Increasing the Ca content, SCCO-8 exhibits finite correlations along both the a and c-axis ( $\xi_c \sim 11 \text{ \AA}$  and  $\xi_a \sim 6 \text{ \AA}$ ). For both compounds, no magnetic correlations were found along the inter-plane direction (b-axis, Fig.1.d). The corresponding Q-dependence of the magnetic intensity along (H,0,1) can be accounted for by an orbital magnetism produced by staggered loop currents (LCs) within the  $\text{CuO}_2$  plaquettes of 2 leg-ladders [8,9]. The result reminds the observation of loop currents confined in charged stripes ladders in lightly doped  $\text{La}_{2-x}\text{Sr}_x\text{CuO}_4$  [10]. While LCs are expected to be absent in hole free ladders, they progressively develop upon hole doping [8,11]. Modeling our data by using two different patterns of LCs nicely captures the main features of our experimental results and give a very small amplitude for the corresponding magnetic moment ( $m \sim 0.05 \mu_B$ ). Our measurements further pinpoint the increase of correlation lengths upon increasing the Ca-content, going along with the development of a magnetic LRO at high Ca-doping. Besides, the LC-like  $q=0$  magnetism appears on Q-positions where scattering from LRO was reported using PND [4-5]. However, no LRO is reported for SCCO-5 and 8,  $T_{\text{mag}} \gg T_N$  (Fig.1.c).

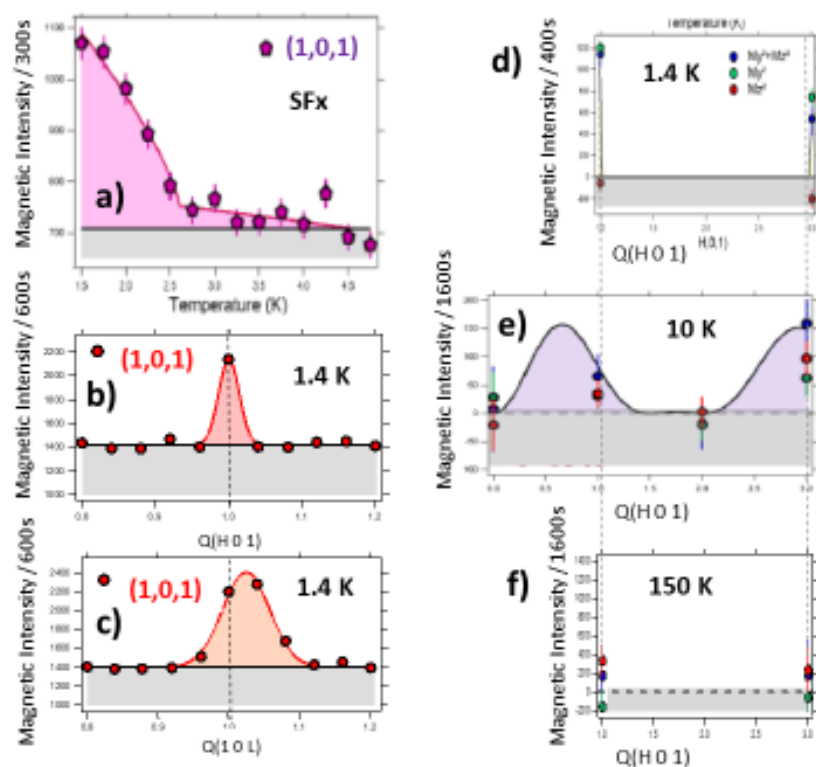


Figure 2 SCCO-12. (a) Temperature dependence of the intensity at the magnetic Bragg peak (1,0,1) giving  $T_N = 2.7 \text{ K}$ . The grey area is the background value estimated from a longitudinal scan, collected at 1.4 K. b-c) H- and L scan across (1,0,7) at 1.4 K in SF channel with neutron polarization along X. (d-f) XYZ-PA of the magnetic scattering along the (H,0,1) line: d) in the LRO-phase at 1.4 K, e) in the LC phase at 10 K, f) in the paramagnetic state at 150 K. Below  $T_N$ , at 1.6 K, the out-of-plane contribution  $M_z^2$  is not sizeable. Above  $T_N$ , at 10 K the L-dependence of the magnetic scattering change and both in-plane ( $M_y^2$ ) and out-of-plane ( $M_z^2$ ) magnetic scatterings are equally balanced. The solid bold line in e) is a fit to the data using a CC-011 like model of LCs within the

### Outcome of Exp CRG-2614.

The experiment was performed on a high quality single crystal of  $(\text{Sr,Ca})_{14}\text{Cu}_{24}\text{O}_{41}$  with  $x_{\text{Ca}} = 12$  (SCCO-12). The crystal was grown using the travelling solvent floating zone method at *Institut de Chimie Moléculaire et des Matériaux d'Orsay*. It is perfectly characterized and exhibits a typical mosaic spread of  $\sim 0.3^\circ$ . It undergoes, on cooling, a magnetic transition to a LRO state, with:  $T_N \sim 2.7 \text{ K}$ , as measured by neutron diffraction consistent with earlier works in literature [12].

The elastic measurements were performed on IN22, equipped with neutron polarization set-up (Heusler/Heusler) and its full polarization analysis device (CRYOPAD). The neutron energy was set to 14.7 meV and a single PG filter was inserted on the scattered beam to remove high contamination. It is worth pointing out that a single PG filter tuned out to be not sufficient to get rid of  $\lambda/2$  Parasitic Bragg scatterings. The sample was aligned in the a-c scattering plane, so that wave vector of the form

(H,0,L) were accessible. In this report, we used the same reduced lattice units as in [1]. The flipping ratio measured on nuclear Bragg reflections (2,0,0) and (0,0,2) was  $\sim 18$  whatever the neutron Polarization direction (X,Y,Z).

The experiment allowed us to confirm the persistence of a LC phase in the SCCO-12 compound. This compound is characterized by the appearance of an AF-LRO below  $T_N \sim 2.7$  K, as shown by the magnetic intensity measured on the (1,0,1) magnetic Bragg reflection (Fig. 2.a). At 1.4K, H- and L-scans (Fig. 2.b-c) around (1,0,1) give  $\xi_a \sim 179$  Å and  $\xi_c \sim 117$  Å for the in-plane and out-of-plane magnetic correlation length. Along the (H,0,1) rod, the magnetic scattering is clearly visible at both H=1 and H=3 (Fig. 2.d). The XYZ polarization analysis indicates that the in-plane magnetic scattering  $M_y^2$  dominates the magnetic signal, while the out-of-plane magnetic response  $M_z^2$  is vanishingly small (Fig. 2.d). This result agrees with magnetic moments parallel to **a**, as reported in the literature. At 10K (above  $T_N$ ), the weak magnetic signal survives at (1,0,1) (Fig. 2.e). The L-dependence of that magnetic signal is at odds that produces by the AF-LRO. Indeed along (H,0,1) rod, the intensity is hardly sizeable at H=1, but remains well defined at H=3. The overall variation of the magnetic scattering is actually consistent with the structure factor of a LC state: the solid line in Fig. 2.e corresponds to the structure factor associated with CC-0II magnetic pattern for LCs within the ladders [6]. In agreement with polarized neutron data, reported for SCCO-5 and SCCO-8 [6],  $M_y^2 \sim M_z^2$ ,  $M_z$ . At very large temperature, the magnetic signal disappears (Fig. 2.f).

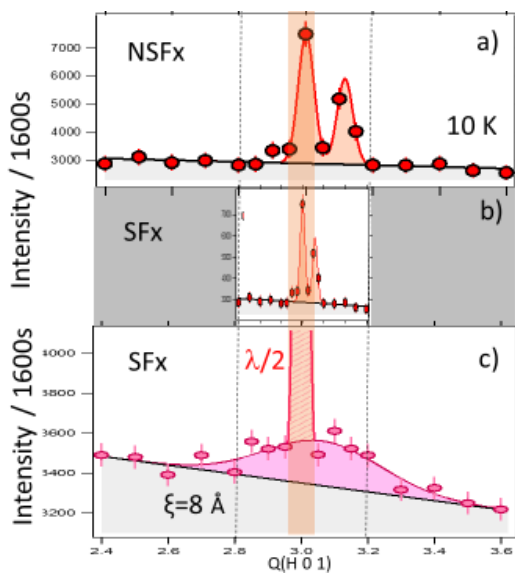


Figure 3 H-scan around (3,0,1) at 10K with the neutron polarization parallel to X: a) in the NSF channel, a-b) in the SF channel with two different scanning ranges.

At Lower Ca content, SCCO-5 and -8, the LC magnetism remains at short range. In SCCO-12, an estimate of the in-plane correlation is made difficult by the strong  $\lambda/2$  contamination that persists with a single PG. filter on the scattered neutron beam. Using Heusler crystals for monochromator and analyzer, the  $\lambda/2$  contaminations remain unpolarized and show up in both NSF and SF channels, as can be seen in Fig. 3.a-b around (3,0,1). Nevertheless, it seems that LC magnetism could be sizeable at the bottom of such the parasitic Bragg scatterings. The broad signal in the SF channel in the tail of the  $\lambda/2$  is consistent with a typical correlation length of  $\sim 8$  Å (Fig. 3.c), suggesting that the LC magnetism is still at rather short range. This result should be confirmed by further measurements with a better  $\lambda/2$  filtration. Meanwhile, additional measurements as a function of temperature suggest an onset temperature  $T_{mag} \sim 65$  K for the LC magnetism.

## References

- [1] M. Uehara et al., *J. Phys. Soc. Jpn.*, **65**(9), 2764 (1996).
- [2] Y. Gotoh et al., *Phys. Rev. B* **68**, 224108 (2003).
- [3] T. Vuletic, et al., *J. Phys. Rep.* **428**(4), 169–258 (2006).
- [4] M. Isobe, M et al., *Phys. Rev. B* **59**(13), 8703 (1999).
- [5] G. Deng, et al., *Phys. Rev. B* **88**(17), 174424 (2013).
- [6] D. Bounoua et al *Commun Phys* **3**, 123 (2020).
- [7]  $\text{Sr}_{14}\text{Cu}_{24}\text{O}_{41}$  crystallizes in an orthorhombic structure (Fig.1.e) The chains and ladders subsystems are described by the orthorhombic space groups *Amma* and *Fmmm*, respectively, that interpenetrate incommensurately along the c-axis with  $10 \times \text{cChains} = 7 \times \text{cLadders}$ . Upon Cdoping, the chain sub-space group changes from *Amma* to *Fmmm* such that the whole structure was described by Deng *et al.*, as belonging to *Xmmm(00g)ss0* superspace group.
- [8] C. M. Varma. *Phys. Rev. B* **73**, 155113 (2006).
- [9] S. Scheurer et al., *Phys. Rev. B* **98**(23), 235126 (2018).
- [10] V. Balédent *et al.*, *Phys. Rev. Lett.* **105**, 027004 (2010).
- [11] P. Chudzinski et al., *Phys. Rev. B* **76**, 161101(R) (2007); *Phys. Rev. B* **78**, 075124 (2008); and *Phys. Rev. B* **81**, 165402 (2010).
- [12] M. Nagate et al., *J. Phys. Soc. Jpn.* **68**(7), 2206-2209 (1999)